Predicting Support Reaction Forces for Standing and Seated Tasks with Given Postures-A Preliminary Study

Brad Howard and Jingzhou (James) Yang

Department of Mechanical Engineering
Texas Tech University, Lubbock, TX 79409, USA
james.yang@ttu.edu

Abstract. This paper proposes a systematic approach for predicting the support reaction forces (SRFs) acting on a digital human model with a given posture. In addition, a generic method has been developed to determine the accurate body segment inertia properties (BSIPs) needed for subject-specific simulation. Experiments based on motion capture are used to track the posture and to find subject's link lengths. The prediction model calculates the support reaction forces by using the zero moment point (ZMP) formulation. This study considers two general postural cases: standing and seated. The standing tasks include standing on two planes with arbitrary orientations. The seated tasks include sitting on a seat where the seat pan is parallel to the floor and both feet are on the floor.

Keywords: Support reaction forces; digital human model; ZMP; posture.

1 Introduction

The advances in the field of digital human modeling (DHM) have allowed researchers to accurately predict human posture and motion while interacting with the environment. One of the major environmental interactions, and long standing problems in DHM, is how to predict the support reaction forces (SRF's) for various standing and seated tasks without measuring them. Traditional methods used to determine the SRFs are based on experiments to measure these forces using forces plates or load cells. However, in the digital human modeling environment, it is impossible to measure the SRFs. Therefore, it is important to accurately predict the SRFs for various standing and seated tasks. To date most DHM models only have the capability to predict SRFs on flat ground. A lot of human tasks such as climbing stairs or standing on uneven terrain are not considered in currently available prediction models. Recent work has extended that capability to predict SRFs acting on a human in a seated position ignoring foot-ground contacts (Kim et al., 2009). However, most seated tasks include those reactions. Therefore, it is necessary for the development of predictions models that include these types of tasks.

Body segment inertia properties (segment mass, centers of mass, and moments of inertia) are important sets of data for any type of biomechanical analysis. Any prediction model using human dynamics that considers human subjects instead of general populations needs subject-specific data including BSIPs. Consequently, it is

V.G. Duffy (Ed.): Digital Human Modeling, HCII 2011, LNCS 6777, pp. 89–98, 2011.

necessary to have a generic method that can estimate these data based on the subject's total body stature and mass.

The objective of this study is to predict the support reaction forces acting on a human in a known posture by (1) developing a method to accurately estimate the body segment inertia properties of specific subjects and (2) creating a prediction model based on the zero moment point formulation that can account for arbitrary support planes while standing, and for seated postures that include foot contacts.

Recently, the static joint torques of a digital human model were calculated in Yang et al. (2009). Yang et al. (2009) also used the ZMP formulation and a linear distribution model to predict ground reaction forces on flat ground. The ZMP formulation can be found in Vukobratović and Borovac (2004) and Goswami et al. (1999). Its coincidence with the center of pressure is described in Sardain and Bessonet (2004). Kim et al. (2009) extended Yang et al. (2009) formulation to include seated reaction forces without considering foot contacts.

Applying these methods to subject-specific models has not yet been done and, as mentioned, needs the addition of subject-specific body segment inertia properties. Dempster (1955) completed a study for the air force that served as a benchmark for many future studies. Since then, many linear and non-linear regression equations have been developed that can estimate the BSIP information given body stature and weight (Zatsiorski et al., 1990, Hatze et al., 1980, McConville et al., 1980, Young et al., 1983, Niklova et al., 2007, Niklova et al., 2010). Many studies recently have improved the regression equations found in these studies so that they apply more to the general population or a specific application (de Leva, 1996, Dumas et al., 2006, Dumas et al., 2007).

This paper is organized as follows. First the kinematics of the human model will be discussed. Next the formulation of the problem will be covered to include estimation of body segment inertia properties, calculation of static joint torques, the zero-moment point formulation, and the SRF prediction model. Examples will then be presented and discussed. Finally conclusion and future work considerations will be offered.

2 Human Model and Kinematics

The human body can be modeled as a kinematic chain consisting of revolute joints representing the musculoskeletal joints and are connected by links that represent the bones. The vector $\mathbf{q} = [q_1 \quad \cdots \quad q_n]^T$ is comprised of the generalized coordinates and represents a unique posture. The position of the end effectors, the hands and the feet, are described by a vector in Cartesian space and is a function of $\mathbf{q}$: $\mathbf{x}(\mathbf{q}) \in R^3$ (Yang et al., 2004). Since the generalized coordinates are measured about the local z axis, transformation matrices are needed for each degree of freedom in order to calculate $\mathbf{x}(\mathbf{q})$. The transformation matrices are found through the use of the Denavit Hartenberg (DH) method (Denavit Hartenberg, 1955). The general form of the matrix can be presented by ${}^{i-1}T_i$. By successively multiplying these matrices together as in Eq. (1), the global coordinates of any point in the mechanism can be calculated.

Likewise, the time derivatives of Eq. (1) will provide the global velocities and acceleration of any point in the mechanism.

$$A_j = T_1 T_2 \cdots T_j = A_{j-1} T_j \tag{1}$$

Human model used in this study is based on the kinematics above and consists of 55 DOF. There are 6 global DOF, 12 spinal DOF, 9 DOF in each arm, 5 DOF in the head and neck, and 7 DOF in each leg.

3 Problem Formulation

The formulations of the different aspects of this study will be covered in this section. The general problem is to find support reaction forces for given subject specific BSIPs and posture $\mathbf{q}$. First the estimation methods for the BSIPs will be briefly introduced. Then the joint torque and ZMP will be discussed, and finally the SRF prediction models will be presented.

3.1 Subject-Specific Body Segment Inertial Properties

The body segment inertial properties of each segment need to be accurately calculated in order to predict or calculate accurate support reaction forces. The method in this study is based on studies from Dumas et al. (2006), and de Leva et al. (1996). **Fig. 1.** and Table 1 show the data collected from these studies (the moments of inertia will not be shown as only static postures are considered in this study).

For segments of the body such as the thigh, shank, forearm, and upper arm, the data from these studies can be used directly. However, some of the data from these studies could not be used directly as certain parts of the body were lumped together. For example, it can be seen in Fig. 1. that the torso includes all spinal segments and. The BSIP data for these segments need to be subject to further decomposition, due to the nature of the human model used for simulation.

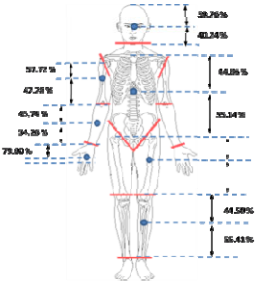

Fig. 1. Center of mass percentages (de Leva et al., 1996)

This decomposition is accomplished by transforming the 50 percentile model into a subject specific model. In order to illustrate this transformation, the decomposition of the torso will be presented. First, the mass percentage of the torso of each individual segment in the torso, $\%m_i^{torso}$, must be calculated.

$$\%m_i^{torso} = m_i / \sum_{i=1}^{9} m_i \tag{2}$$

$m_i \ (i = 1,2,...,9)$ is the individual mass of each segment in the torso. Next the mass percentage of the total body mass of each individual segment in the torso, $\%m_i^{total}$, must be found. This is calculated using the data in Table 1 .

$$\%m_i^{total} = \%m_i^{torso} \times 33.3\% \tag{3}$$

Table 1. Segment mass

Body Segment	*Mass (%)*
Head and Neck	6.7
Torso	33.3
Arm	2.4
Forearm	1.7
Hand	0.6
Pelvis	14.2
Thigh	12.3
Shank	4.8
Foot	1.2

Now the mass of the individual torso segments of any subject can be calculated from the subjects body mass, $m_{subject}$, recorded during the experiment.

$$m_i = m_{subject} \times \%m_i^{total} \tag{4}$$

The center of mass for each segment was estimated to be at 50% of the segment length. This brought the estimated center of mass for the whole torso very close to that found in Fig. 1.

3.2 Joint Torque and ZMP

Joint torque is realized through the backward recursive dynamic formulation (Yang et al., 2009). The ZMP is defined as the point on the ground in which the tipping moments due to the reaction forces are zero. The reaction forces at the ZMP, F^{ZMP} and M^{ZMP}, can then be calculated (Yang et al., 2009). It is important to note that P_{ZMP} should coincide with the center of pressure (CoP) (Sardain and Bessonet, 2004). And, since the postures are static, the CoP/ZMP should be a projection of the center of mass of the body on the ground or support plane. Because the SRF distribution is based on the ZMP position, human models, specifically the BSIPs and body segment length, are required to be subject-specific.

3.3 Support Reaction Forces

The support reaction force prediction model is formulated in this section. Generally, it is a linear distribution based on the distance between the application of the SRFs and P_{ZMP}, Newton's first law, and the angles of the support planes. The distribution model can be organized into two cases: the standing case (two-force distribution) and the seated case (four-force distribution).

Before the actual prediction model is presented, the application of Newton's first law will be explained. Fig. 2. is schematic that shows the distribution of F^{ZMP} and M^{ZMP} to the two feet (F^R, F^L, M^R, and M^L) where D^R and D^L are the distance vectors from the ZMP to the application points P_R and P_L.

$$F_y^R = \frac{D_x^L + D_z^L}{D_x^R + D_z^R + D_x^L + D_z^L} F_y^{ZMP}; F_y^L = \frac{D_x^R + D_z^R}{D_x^R + D_z^R + D_x^L + D_z^L} F_y^{ZMP} \tag{5}$$

Eq. (5) only shows the model for one component in a general two forces case but the method is applied for the other two components. This model provides the basis for all the prediction models.

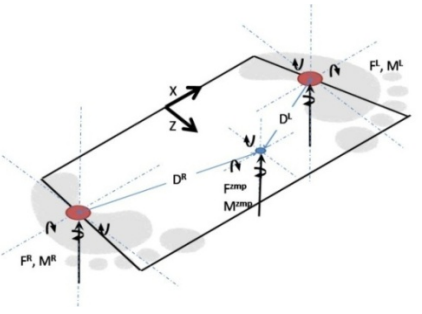

Fig. 2. General schematic for two-SRF distribution

(1) General Standing Case

The general standing case is a two force distribution between the right and left feet. The distribution is compensated by using cosines of the support plane angle:

$$F_y^R = \frac{(D_x^L + D_z^L)\cos^2\alpha}{(D_x^R + D_z^R)\cos^2\beta + (D_x^L + D_z^L)\cos^2\alpha} F, F_x^R = \frac{(D_y^L + D_z^L)\cos^2\alpha}{(D_y^R + D_z^R)\cos^2\beta + (D_y^L + D_z^L)\cos^2\alpha} F_x^{ZMP}$$
$$F_z^R = \frac{(D_x^L + D_y^L)\cos^2\alpha}{(D_x^R + D_y^R)\cos^2\beta + (D_x^L + D_y^L)\cos^2\alpha} F_z^{ZMP} \tag{6}$$

$$F_y^L = \frac{(D_x^R + D_z^R)\cos^2\beta}{(D_x^R + D_z^R)\cos^2\beta + (D_x^L + D_z^L)\cos^2\alpha} F_y^{ZMP}, F_x^L = \frac{(D_y^R + D_z^R)\cos^2\beta}{(D_y^R + D_z^R)\cos^2\beta + (D_y^L + D_z^L)\cos^2\alpha} F_x^{ZMP}$$
$$F_z^L = \frac{(D_x^R + D_y^R)\cos^2\beta}{(D_x^R + D_y^R)\cos^2\beta + (D_x^L + D_y^L)\cos^2\alpha} F_z^{ZMP} \tag{7}$$

α is the angle of the right foot support plane and β is angle of the left foot support plane and can be seen in Fig. 3.

The moment vectors of the SRF are then calculated using the same distribution scheme. However distribution of the moment also requires the parallel axis theorem:

$$M_y^R = \frac{(D_x^L + D_z^L)\cos^2\alpha}{(D_x^R + D_z^R)\cos^2\beta + (D_x^L + D_z^L)\cos^2\alpha} M_y^{ZMP} + (D^R \times F^R)\vec{j}, M_x^R = \frac{(D_y^L + D_z^L)\cos^2\alpha}{(D_y^R + D_z^R)\cos^2\beta + (D_y^L + D_z^L)\cos^2\alpha} M_x^{ZMP} + (D^R \times F^R)\vec{i}$$
$$M_z^R = \frac{(D_x^L + D_y^L)\cos^2\alpha}{(D_x^R + D_y^R)\cos^2\beta + (D_x^L + D_y^L)\cos^2\alpha} M_z^{ZMP} + (D^R \times F^R)\vec{k} \tag{8}$$

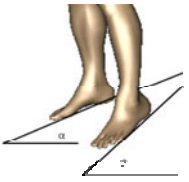

Fig. 3. Visual representation of α and β

(2) General Seated Case

The seated case becomes more complicated because there are four points of contact to which the SRF's have to be distributed. This study only considers a seat pan parallel to the floor. The cosine functions used in the distribution will go to 1 as the angles are zero. The general template derived in (5) can still be followed, however another step must be added. Basically, two 2-force distribution models will be used in series. First the loads at the ZMP will be distributed between the seat pan and the floor. Fig. 4. shows the location of the points of distribution (P^{SP} and P^{F}) for the seat pan and the floor, where D^{T} and D^{F} are the vectors from the ZMP to the thigh and foot application points, respectively. $D^{RT}, D^{LT}, D^{RF}, D^{LF}$ are the distance vectors between the intermediate application points and the end application points. These vectors can be seen in Fig. 4.

The equations for the distribution are as follows:

$$F_y^T = \frac{(D_x^F + D_z^F)}{(D_x^T + D_z^T) + (D_x^F + D_z^F)} F_y^{ZMP}, F_x^T = \frac{(D_y^F + D_z^F)}{(D_y^T + D_z^T) + (D_y^F + D_z^F)} F_x^{ZMP}$$
$$F_z^T = \frac{(D_x^F + D_z^F)}{(D_x^T + D_y^T) + (D_x^F + D_y^F)} F_z^{ZMP} \tag{9}$$

$$F_y^F = \frac{(D_x^T + D_z^T)}{(D_x^T + D_z^T) + (D_x^F + D_z^F)} F_y^{ZMP}, F_x^F = \frac{(D_y^T + D_z^T)}{(D_y^T + D_z^T) + (D_y^F + D_z^F)} F_x^{ZMP}$$
$$F_z^F = \frac{(D_x^T + D_y^T)}{(D_x^T + D_y^T) + (D_x^F + D_y^F)} F_z^{ZMP} \tag{10}$$

Once the loads are distributed to P^{SP} and P^{F}, they can be distributed again to the points of contact (P^{RT}, P^{LT}, P^{RF}, and P^{LF}). That is accomplished through another two force distribution:

$$F_y^{RT} = \frac{(D_x^{LT} + D_z^{LT})}{(D_x^{RT} + D_z^{RT}) + (D_x^{LT} + D_z^{LT})} F_y^T, F_x^{RT} = \frac{(D_y^{LT} + D_z^{LT})}{(D_y^{RT} + D_z^{RT}) + (D_y^{LT} + D_z^{LT})} F_x^T$$
$$F_z^{RT} = \frac{(D_x^{LT} + D_y^{LT})}{(D_x^{RT} + D_y^{RT}) + (D_x^{LT} + D_y^{LT})} F_z^T \tag{11}$$

$$F_y^{RF} = \frac{(D_x^{LF} + D_z^{LF})}{(D_x^{RF} + D_z^{RF}) + (D_x^{LF} + D_z^{LF})} F_y^F, F_x^{RF} = \frac{(D_y^{LF} + D_z^{LF})}{(D_y^{RF} + D_z^{RF}) + (D_y^{LF} + D_z^{LF})} F_x^F$$
$$F_z^{RF} = \frac{(D_x^{LF} + D_y^{LF})}{(D_x^{RF} + D_y^{RF}) + (D_x^{LF} + D_y^{LF})} F_z^F \tag{12}$$

Substituting equations (9) and (10) into (11) and (12) respectively, the full distribution prediction model can be calculated. $Rate_{n_i}^{\text{Application Point}}$ will be use as the

template to call the intermediate distribution models for clarity, where $\vec{n_i}$ $(i = 1, 2, 3)$ denotes the global x y or z unit vectors, respectively. The full general prediction models are as follows:

$$F_{\vec{n_i}}^{RT} = Rate_{\vec{n_i}}^{RT} Rate_{\vec{n_i}}^{SP} F_{\vec{n_i}}^{ZMP}, F_{\vec{n_i}}^{LT} = Rate_{\vec{n_i}}^{LT} Rate_{\vec{n_i}}^{SP} F_{\vec{n_i}}^{ZMP} \tag{13}$$

$$F_{\vec{n_i}}^{RF} = Rate_{\vec{n_i}}^{RF} Rate_{\vec{n_i}}^{F} F_{\vec{n_i}}^{ZMP}, F_{\vec{n_i}}^{LF} = Rate_{\vec{n_i}}^{LF} Rate_{\vec{n_i}}^{F} F_{\vec{n_i}}^{ZMP} \tag{14}$$

The moment vectors of SRF follow the same model but include the parallel axis theorem:

$$\begin{aligned} M_{\vec{n_i}}^{RT} &= Rate_{\vec{n_i}}^{RT} Rate_{\vec{n_i}}^{SP} M_{\vec{n_i}}^{ZMP} + [(D^T + D^{RT}) \times F^{RT}] \cdot \vec{n_i} \\ M_{\vec{n_i}}^{LT} &= Rate_{\vec{n_i}}^{LT} Rate_{\vec{n_i}}^{SP} M_{\vec{n_i}}^{ZMP} + [(D^T + D^{LT}) \times F^{LT}] \cdot \vec{n_i} \end{aligned} \tag{15}$$

$$\begin{aligned} M_{\vec{n_i}}^{RF} &= Rate_{\vec{n_i}}^{RF} Rate_{\vec{n_i}}^{F} M_{\vec{n_i}}^{ZMP} + [(D^F + D^{RF}) \times F^{RF}] \cdot \vec{n_i} \\ M_{\vec{n_i}}^{LF} &= Rate_{\vec{n_i}}^{LF} Rate_{\vec{n_i}}^{F} M_{\vec{n_i}}^{ZMP} + [(D^F + D^{LF}) \times F^{LF}] \cdot \vec{n_i} \end{aligned} \tag{16}$$

Note that when the distance vectors are used in the distribution model, the magnitude is used and the direction is ignored for the numeric simplicity.

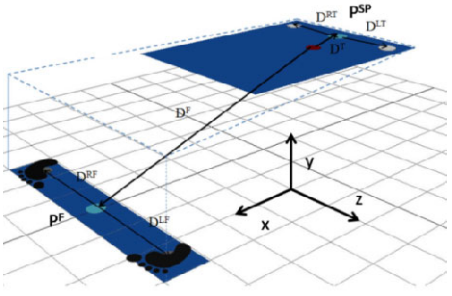

Fig. 4. General schematic for the seated case

4 Simulation Examples

The results of the simulations are presented in this section. There are four different tasks applied to two different postural orientation cases. The orientation cases are: standing with each foot on an angled plane (uneven terrain), and seated on a ground parallel seat pan with feet on the ground.

(1) Standing Case

The support plane angles α and β were selected to be 0 and 15 degrees respectively for the standing case. The results for four different tasks will now be presented.

The SRFs predicted for each of the tasks in Fig. 5 can be found below in Table 2.

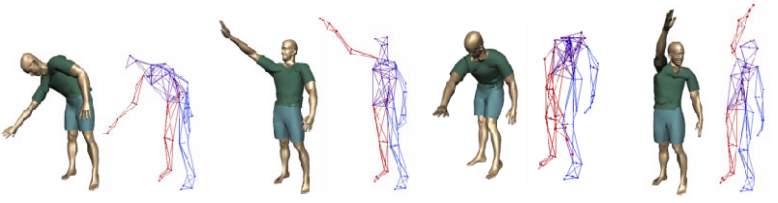

(a) Task 1 (b) Task 2 (c) Task 3 (d) Task 4

Fig. 5. Visualization of the predicted postures for each task

Table 2. SRF for standing all Tasks

		SRF					
		Force Vector (N)			Moment Vector (N-m)		
		x	y	z	x	y	z
Task 1	Right Foot	0	552.005	0	16.456	0	32.989
	Left Foot	0	138.841	0	4.06614	0	-43.423
Task 2	Right Foot	0	485.278	0	8.716	0	59.1513
	Left Foot	0	205.569	0	12.67	0	-52.519
Task 3	Right Foot	0	122.59	0	-2.86	0	39.119
	Left Foot	0	568.255	0	-1.838	0	-38.489
Task 4	Right Foot	0	219.69	0	-0.43353	0	60.275
	Left Foot	0	471.15	0	14.501	0	-43.8107

4.1 Seated Case

The seated case had four tasks as well but they were repositioned so that they were reachable from seated position. There is only one postural orientation for the seated case. The SRF's for all four seated tasks are shown in Table 3.

Table 3. SRF for all four tasks in the seated case

		SRF					
		Force Vector			Moment Vector		
		x	y	z	x	y	z
Task 1	Right Thigh	0	333.0565	0	-42.1194	0	20.049
	Left Thigh	0	134.9282	0	-15.23	0	-24.578
	Right Foot	0	155.233	0	36.79	0	26.896
	Left Foot	0	67.629	0	17.84	0	-25.09
Task 2	Right Thigh	0	295.89	0	-34.22	0	28.002
	Left Thigh	0	192.187	0	-19.72	0	-30.87
	Right Foot	0	131.378	0	32.45	0	25.501
	Left Foot	0	71.393	0	17.515	0	-25.384
Task 3	Right Thigh	0	33.675	0	-4.056	0	7.432
	Left Thigh	0	420.242	0	-54.436	0	-7.739
	Right Foot	0	58.429	0	14.5	0	24.858
	Left Foot	0	178.5	0	42.91	0	-23.468
Task4	Right Thigh	0	28.41	0	-2.524	0	6.447
	Left Thigh	0	430.22	0	-53.4322	0	-7.45
	Right Foot	0	41.772	0	10.246	0	19.099
	Left Foot	0	190.446	0	45.866	0	-18.251

4.2 Discussion

The SRFs predicted from the simulations can all be considered logical or realistic. They follow the general trends that would be expected from the postural orientations

that were required to complete the tasks. The ZMP positions of each of the tasks were not shown even though the force distribution is a direct reflection its value. This data was not presented because of the nature of given postures. The given postures were found through the posture reconstruction of motion capture data. The locations of the feet, though realistically were identical for all tasks, were calculated to be different in the reconstruction because it assumes that the hip point is at the origin. This renders the comparison of ZMP locations between tasks ineffectual and does not reflect the difference in postural stability or SRF distribution across the postural orientations.

One aspect that is important to note is the relationship between the body segment inertia properties and the calculated support reaction forces. For any given trial the summation of the vertical component of the SRF force vector provided a total force of 690.846 N. When dividing by the acceleration of gravity, the total mass of the DHM is calculated to be 70.42 kg. When the subject was weighed in before the experiment, he registered 155 lbs or 70.32 kg. The means that the body mass of the subject was estimated to .142% of the actual body mass; an error that is definitely acceptable.

5 Conclusions and Future Work

This paper presented a method for predicting support reaction forces from known posture found in motion capture experimentation. Also presented was a generic method for determining the body segment inertia properties for specific subjects used in experimentation. Based on these methods, experiments in motion capture and simulations were run in order to test the methods presented. The SRF force predicted followed the general trends expected from the capture and provided realistic values. The body segment inertial property estimation provided a body mass with the .142% error. Validation for the SRF prediction model is needed to evaluate the accuracy of the predicted loads.

Overall the proposed methodology presented in this paper is sound. It provides the ability to predict SRFs for general cases. As mentioned in the discussion portion of this paper, it is important to define accurate location of application for the reaction forces. The addition of pressure mapping system in the validation of the model presented in this paper would be very useful.

Acknowledgments. This research work was partly supported by National Science Foundation (Award # 0926549).

References

1. Denavit, J., Hartenberg, R.S.: A Kinematic Notation for Lower-Pair Mechanisms Based on Matrices. Journal of Applied Mechancis 22, 215–221 (1955)
2. Fujimaki, G., Mitsuya, R.: Study of the Seated Posture for VDT Work. Displays 23(1-2), 17–24 (2002)
3. Goswami, A.: Postural Stability of Biped Robots and the Foot Rotation Indicator (FRI) Point. International Journal of Robotics Research 18(6) (1999)
4. Kim, J., Yang, J., Abdel-Malek, K.: Multi-objective Optimization Approach for Predicting Seated Posture Considering Balance. International Journal of Vehicle Design 51(3/4), 278–291 (2009)

5. Sardain, P., Bessonnet, G.: Forces Acting on a Biped Robot. Center of Pressure-Zero Moment Point. IEEE Transactions on Systems, Man and Cybernetics Part A 34(5), 630–637 (2004)
6. Vukobratović, M., Borovac, B.: Zero-moment Point–Thirty Five Years of its Life. International Journal of Humanoid Robotics 1(1), 157–173 (2004)
7. Yang, J., Xiang, Y., Kim, J.: Determining the Static Joint Torques of Digital Human Models Considering Balance. In: ASME 2009 International Design Engineering Technical Conference, San Diego California (2009)
8. Hatze, H.: A Mathematical Model for the Computational Determination of Parameter Values of Anthropomorphic Segments. Journal of Biomechanics 13(10), 833–843 (1980)
9. Yang, J., Marler, T., Kim, H.J., Arora, J., Abdel-Malek, K.: Multi-Objective Optimization for Upper Body Posture Prediction. In: 10th AIAA/ISSMO Multidesicinplinary Analysis and Optimization Conference, Albany, New York (2004)
10. Zatsiorsky, V., Seluyanov, V., Chugunova, L.G.: Methods of Determining Mass-Inertial Characteristics of Human Body Segments. In: Chernyi, G.G., Regirer, S.A. (eds.) Contemporary Problems of Biomechanics, pp. 272–291. CRC Press, Boston (1990)
11. Dempster, W.T.: Space Requirements for the Seated Operator. WADC Technical Report TR-55-159, Wright Air Development Center, Wright–Patterson Air Force Base, Dayton, Ohio (1955)
12. de Leva, P.: Adjustments to Zatsiorsky–Seluyanov's Segment Inertia Parameters. Journal of Biomechanics 29, 1223–1230 (1996)
13. McConville, J.T., Churchill, T.D., Kaleps, I., Clauser, C.E., Cuzzi, J.: Anthropometric Relationships of Body and Body Segment Moments of Inertia. Technical Report AFAMRL-TR-80-119, Aerospace Medical Research Laboratory, Wright–Patterson Air Force Base, Dayton, Ohio (1980)
14. Young, J.W., Chandler, R.F., Snow, C.C., Robinette, K.M., Zehner, G.F., Lofberg, M.S.: Anthropometric and Mass Distribution Characteristics of Adult Females. Technical ReportFA-AM-83-16, FAA Civil Aeromedical Institute, Oklahoma City, Oklahoma (1983)
15. Nikolova, G., Toshev, Y.: Estimation of Male and Female Body Segment Parameters of the Bulgarian Population Using a 16-segmental Mathematical Model. Journal of Biomechanics 40, 3700–3707 (2007)
16. Nikolova, G.: Anthropometric Measurements and Model Evaluation of Mass-Inertial Parameters of the Human Upper and Lower Extremities. In: IFMBE Proceedings, vol. 29, pp. 574–577 (2010)
17. Dumas, R., Cheze, L., Verriest, J.P.: Adjustments to McConville et al. and Young et al. Body Segment Inertial Parameters. Journal of Biomechanics 40, 543–553 (2006)
18. Dumas, R., Cheze, L., Verriest, J.P.: Corrigendum to "Adjustments to McConville et al. and Young et al. Body Segment Inertial Parameters" [J. Biomech. 40 (2007) 543–553]. Journal of Biomechanics 40, 1651–1652 (2006)
19. Gragg, J., Yang, J.: Posture Reconstruction for Digital Human Models - Methodology Study. Ergonomics (2010) (submitted)